Nuclear Engineering and Technology 54 (2022) 917–925

Contents lists available at ScienceDirect

Nuclear Engineering and Technology

journal homepage: www.elsevier.com/locate/net

Original article

Modified θ projection model-based constant-stress creep curve for alloy 690 steam generator tube material

Seongin Moon [a, *], Jong-Min Kim [a], Joon-Yeop Kwon [a], Bong-Sang Lee [a], Kwon-Jae Choi [a], Min-Chul Kim [a], Sangbae Han [b]

[a] Korea Atomic Energy Research Institute, Daejeon, 34057, South Korea
[b] Dassault Systemes Korea, Seoul, 06164, South Korea

ARTICLE INFO

Article history:
Received 3 May 2021
Received in revised form
6 September 2021
Accepted 7 September 2021
Available online 8 September 2021

Keywords:
Creep
Theta projection method
Alloy 690
Steam generator tube
Constant-stress creep curve
Creep hardening rule

ABSTRACT

Steam generator (SG) tubes in a nuclear power plant can undergo rapid changes in pressure and temperature during an accident; thus, an accurate model to predict short-term creep damage is essential. The theta (θ) projection method has been widely used for modeling creep-strain behavior under constant stress. However, many creep test data are obtained under constant load, so creep rupture behavior under a constant load cannot be accurately simulated due to the different stress conditions. This paper proposes a novel methodology to obtain the creep curve under constant stress using a modified θ projection method that considers the increase in true stress during creep deformation in a constant-load creep test. The methodology is validated using finite element analysis, and the limitations of the methodology are also discussed. The paper also proposes a creep-strain model for alloy 690 as an SG material and a novel creep hardening rule we call the damage-fraction hardening rule. The creep hardening rule is applied to evaluate the creep rupture behavior of SG tubes. The results of this study show its great potential to evaluate the rupture behavior of an SG tube governed by creep deformation.

1. Introduction

In a design-basis accident at a nuclear power plant, the temperature change of a steam generator (SG) tube is almost negligible because it is maintained below 350 °C. At this temperature, the creep effect can be ignored in Alloy 690, often used as an SG tube material. However, a much higher temperature can be generated in a severe accident. Extensive plastic deformation is more likely at high temperatures than at the normal operating temperature of a nuclear power plant. Hence, the creep effect can no longer be disregarded [1–5].

Creep is an irreversible time-dependent nonlinear deformation process: the strain depends on both the temperature and time, rather than only on the stress. Generally, creep in metals starts when the temperature is above 0.3–0.4 of the melting temperature [6,7]. The most common method of creep testing is the simple application of a load (or constant engineering stress). With this method, the creep curve can be characterized by three stages [6–8]: the primary stage, where the creep strain increases initially although the strain rate decreases with time; the secondary stage, where the strain rate remains constant; and the tertiary stage, where the strain rate increases rapidly, and creep failure occurs. The steady-state creep rate is known to have a power dependence on stress known as the power-law creep and has an exponential temperature dependence [6–8].

Various constitutive models have been developed to predict and interpolate the creep behavior for the primary, secondary, and tertiary stages of the creep process [8–14]. Modeling all three stages might not be of interest to industrial structure designers; however, it is crucial for SG tube integrity assessment for a hypothetical severe accident, such as a station blackout (SBO) with a loss of auxiliary feedwater. SBO results in turbine-driven auxiliary feedwater (AFW) pump failure, and this sequence typically lead to core damage [2]. As core damage progresses, the temperature and pressure in the primary side of SG increase. The rate of accident progression depends on plant specific design features such as the impact of stuck-open safety valves (SVs), atmospheric dump valves (ADVs), and steam safety valves (MSSVs) and so on. The secondary side of SG could be depressurized as a result of several mechanisms such as stuck-open ADVs and MSSVs and so on. Under SBO, SG

* Corresponding author.
E-mail address: simoon21c@kaeri.re.kr (S. Moon).

https://doi.org/10.1016/j.net.2021.09.008

tubes could undergo rapid changes in pressure and temperature, and the creep damage accumulates within only several hours or days [15,16]. Therefore, there is a need for creep models that can accurately simulate the entire creep curve and evaluate the creep-strain rate transitions under various accident scenarios.

Moreover, SG tubes are generally made of alloy 600; however, the material has been replaced with alloy 690, a Ni–Cr–Fe alloy, with a Cr content of up to 30 wt% to improve its corrosion resistance [17,18]. Most of the studies on creep characteristics and failures of SG tubes have been on alloy 600 materials. Argonne National Laboratory used the alloy 600 material and employed the Larson–Miller method, widely used for simple calculations. However, there have been only a few studies on alloy 690. Creep data are insufficient to predict the creep behavior of SG tubes made of alloy 690.

The θ projection method [6,19] is known to model the shape of the entire creep curve accurately. It can be used to interpolate and extrapolate the creep rate for the stress, strain, and temperature of various alloys. Furthermore, it has been modified extensively for application to various materials [8,12,20–22]. Many researchers have presented a creep curve fitting method using the original and modified θ projection methods. Fu et al. [12] have been proposing an interesting modified θ projection method that considers changes in the actual stress during the creep test under a constant load. Also, the modified method can be applied to obtain the constant-stress creep curve from the constant-load creep curve. The verification was, however, not implemented.

This study proposes a novel creep-strain model for alloy 690 SG tube material, based on the θ projection method, which can represent all three stages of the creep process. Furthermore, a novel creep hardening rule is proposed. The creep hardening rule and the creep-strain model for alloy 690 are applied to evaluate the creep rupture behavior of SG tubes. The utility of the rule and model is validated by comparison with creep rupture test results for SG tubes.

2. Creep-strain model for alloy 690 under constant load

The θ projection method is a creep-modeling method. The creep strain, ε, at time t can be calculated using the following equation:

$$\varepsilon = \theta_1\left(1 - e^{-\theta_2 t}\right) + \theta_3\left(e^{\theta_4 t} - 1\right), \tag{1}$$

where θ_i (i = 1, 2, 3, 4) are the four θ coefficients obtained from a regression analysis of the experimental creep curves. For isotropic materials, the model parameters, $\ln\theta_i$, can be assumed to be a linear function of temperature, T, and stress, σ, as follows:

$$\ln\theta_i = a_i + b_i\sigma + c_i T + d_i\sigma T, \tag{2}$$

where a_i, b_i, c_i, and d_i ($i = 1, \ldots, 4$) are the material constants. In the θ projection method, the definition of the creep strain and stress are dependent on the type of creep curve used for curve fitting: true values for constant-stress creep curves and engineering values for constant-load creep curves.

Our previous study [23] proposed a creep-strain model for alloy 690 for creep curves under constant-load conditions using a modified θ projection method. In our creep test of alloy 690 under a constant load, a series of creep tests was conducted in the temperature range of 650–850 °C. The chemical composition of alloy 690 is given in Table 1, and the geometry and dimensions of the test specimens are shown in Fig. 1. A master curve was proposed through appropriate normalization of creep curves to minimize the temperature and stress dependence between creep curves, as shown in Fig. 2. Then the creep-strain model for alloy 690 under the constant-load condition is as follows:

Table 1
Chemical composition of alloy 690 SG tube material.

Element	C	Mn	SI	S	P	Ni	Cr	Mo
wt.%	0.020	0.493	0.265	0.0006	0.005	59/16	29.27	0.028
Element	Cu	Co	Al	Ti	Nb	N	B	Fe
wt.%	0.012	<0.010	0.165	0.245	<0.010	0.020	<0.0005	10.3

Table 2
Optimized θ coefficients for the master curve of constant-load creep curves for alloy 690 SG material.

θ_1	θ_2	θ_3	θ_4	θ_5
2.45	0.22	0.06	2.32	4.95

$$\varepsilon = \theta_1\left(1 - e^{-\theta_2 t}\right) + \theta_3\left(e^{\theta_4 t^{\theta_5}} - 1\right) \tag{3}$$

The θ parameters are presented in Table 2. Following the determination of the θ values, the $\theta^{T,\sigma}$, for a specific temperature, T, and stress, σ, can be determined using the reference rupture strain, ε_{rr}, and reference rupture time, t_{rr}.

$$\theta_{1,3}^{T,\sigma} = \varepsilon_{rr}\cdot\theta_{1,3};\ \theta_2^{T,\sigma} = \frac{\theta_2}{t_{rr}};\ \theta_4^{T,\sigma} = \frac{\theta_4}{t_{rr}^{\theta_5}};\ \theta_5^{T,\sigma} = \theta_5, \tag{4}$$

$$\ln t_{rr} = 26.399 + 4.097\times10^{-2}\sigma - 2.486\times10^{-2}T - 1.018\times10^{-4}\sigma T, \tag{5}$$

$$\ln\varepsilon_{rr} = 1.875 - 2.088\times10^{-2}\sigma - 4.113\times10^{-3}T + 3.453\times10^{-5}\sigma T \tag{6}$$

Fig. 3 illustrates the comparison of the creep curves predicted using the proposed creep-strain model and the experimental data. The predicted curves show all three-stage creep processes; it can be seen that the predicted and experimental results are in good agreement under the tested temperature and stress conditions except for some cases. The red shaded region bounded by two red dashed lines in Fig. 3(b) indicates the ±20% prediction error intervals in the creep time for the case of 100 MPa; this case shows a relatively large prediction error. The error was occurred during the regression process to drive for Eqs. (5) and (6).

3. Modified θ projection method for constant-stress creep curve

The primary, secondary, and tertiary creep stages can be calculated using the original θ projection method described by Eqs. (1) and (2) at various stresses and temperatures. Those equations can be applied for creep-strain curves under constant-load conditions to approximate the creep strain in a practical application. It is, however, not sufficient to model the creep behavior of structures through finite element analysis (FEA), and the creep curves under constant stress are necessary rather than ones under constant load. Unfortunately, many conventional creep tests are carried out under constant-load conditions [6,12]. The constant-load creep tests cannot consider a decrease of the cross-sectional area of the creep specimens, which leads to a continuously increasing true stress, resulting in significant differences in the actual creep curves under constant stress. Fu et al. [6] have proposed a modified θ projection method that can precisely describe the creep curves obtained under constant load. The modified method considers the increasing true

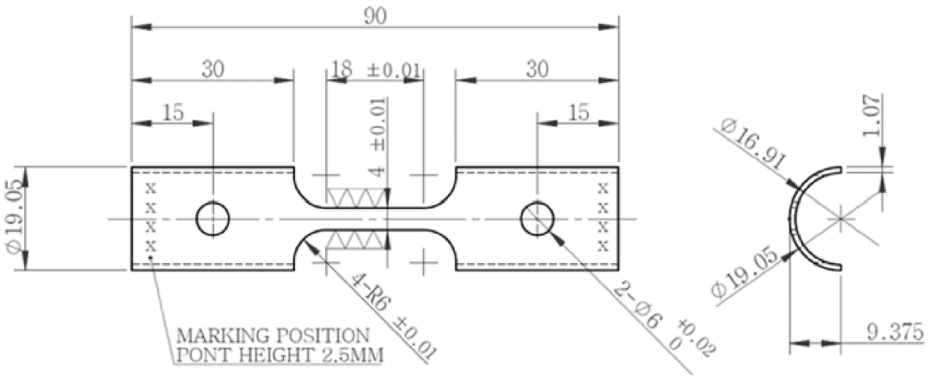

Fig. 1. Geometry and dimensions of creep specimen.

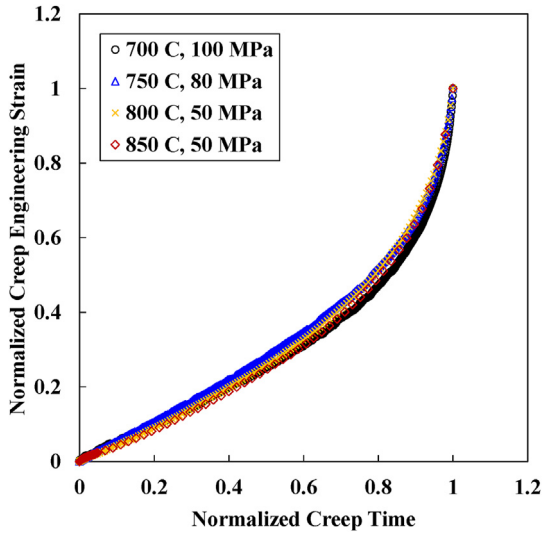

Fig. 2. Normalized creep curves for stress and temperature change by reference creep time and strain.

creep stress under constant load. Also, the modified model was used to predict the creep curves obtained under constant stress from ones under constant load, but the verification was not implemented.

Equation (1) consists of two exponential terms: the first term, $\theta_1(1 - e^{-\theta_2 t})$, represents a decaying primary component, where θ_1 is a scale parameter for primary creep strain, and θ_2 is quantification parameter related to the primary creep-strain rate. Similarly, the second term, $\theta_3(e^{\theta_4 t} - 1)$, represents an accelerating tertiary component with θ_3, which scales the tertiary creep strain, and θ_4, which determines the tertiary creep-strain rate. Fig. 4 is a schematic diagram showing the physical significance of the four θ coefficients. Fu et al. [6] assumed that θ_1 and θ_3 are determined at the beginning of the creep test and remain unchanged throughout the creep process. They also assumed that θ_2 and θ_4 are controlled by the creep-strain rate and may change with the increase in the creep stress. The authors modified Eq. (2) to reflect the nature of the θ_1 and θ_3 parameter as follows:

$$\ln\theta_i = a_i + b_i\sigma_0 + c_iT + d_i\sigma_0 T \ (i = 1,\ 3), \tag{7}$$

$$\ln\theta_i = a_i + b_i\sigma + c_iT + d_i\sigma T \ (i = 2,\ 4), \tag{8}$$

where σ_0 is the initial stress of the constant-load creep test (or creep engineering stress), and σ is the true creep stress which is expressed as follows:

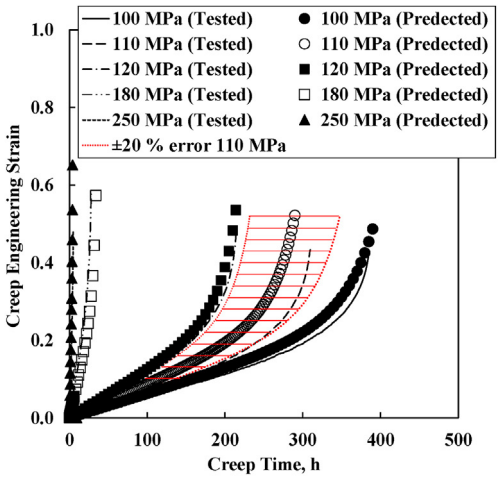

Fig. 3. Example of creep-strain prediction results: (a) 700 °C (b) 800 °C.

$$\sigma = \sigma_0(1 + \varepsilon_0), \tag{9}$$

where ε_0 is the engineering strain. This equation is satisfied under the assumption that the volume of the specimen does not change

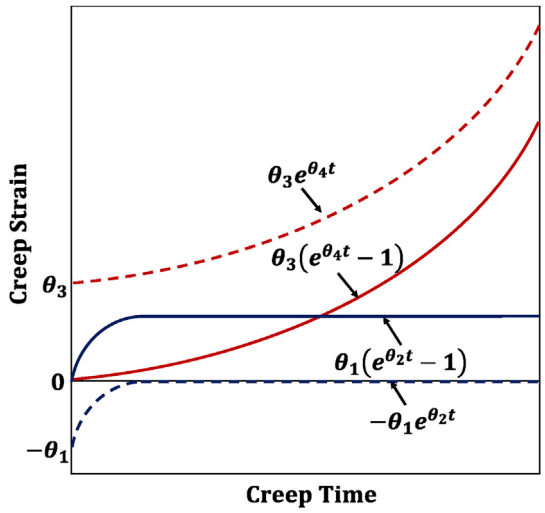

Fig. 4. Schematics representing the physical meaning of θ parameters.

during creep deformation; the true stress, σ, is directly related to the engineering stress, σ_0, and engineering strain, ε_0. This relationship is effective before the onset of necking.

However, we insist that the assumption, which is the values of θ_1 and θ_3 are determined at the beginning of the creep test and remain unchanged throughout the creep process, is not appropriate. All the θ parameters cannot be determined in the middle of the creep process; they can only be determined from the final creep curve. Therefore, we proposed the following new form of Eq. (2):

$$\ln\theta_i = a_i + b_i\sigma + c_iT + d_i\sigma T \ (i=1,\ \ldots,\sim 4) \tag{10}$$

By substituting Eq. (9) in (10), the effect of increasing in creep true stress can be described, and the four θ parameters are then given by:

$$\ln\theta_i = a_i + b_i\sigma_0(1+\varepsilon_0) + c_iT + d_i\sigma_0(1+\varepsilon_0)T \ (i=1\sim 4) \tag{11}$$

Equation (11) can be simply expressed as

$$\ln\theta_i = e_i + f_i\sigma_0(1+\varepsilon_0) \ (i=1,\ \ldots,\sim 4), \tag{12}$$

where e_i and f_i are $a_i + c_iT$ and $b_i + d_iT$, respectively.

Substituting Eq. (12) in Eq. (1), the θ projection model can be expressed as:

$$\varepsilon_0 = e^{e_1+f_1\sigma_0(1+\varepsilon_0)}\left(1-e^{-e^{e_2+f_2\sigma_0(1+\varepsilon_0)}t}\right) + e^{e_3+f_3\sigma_0(1+\varepsilon_0)}\left(e^{e^{e_4+f_4\sigma_0(1+\varepsilon_0)}t}-1\right) \tag{13}$$

This equation describes the creep curve obtained constant-load conditions. The outside parentheses in the first term in Eq. (13) can be further simplified as follows:

$$e^{e_1+f_1\sigma_0(1+\varepsilon_0)} = e^{e_1+f_1\sigma_0+f\sigma_0\varepsilon_0} = \theta_1 e^{f\sigma_0\varepsilon_0} = \theta_1 e^{A\varepsilon_0} \tag{14}$$

Similarly, the others in Eq. (13) can be written as:

$$e^{e_2+f_2\sigma_0(1+\varepsilon_0)} = \theta_2 e^{B\varepsilon_0};\ e^{e_3+f_3\sigma_0(1+\varepsilon_0)} = \theta_3 e^{C\varepsilon_0};\ e^{e_4+f_4\sigma_0(1+\varepsilon_0)} = \theta_4 e^{D\varepsilon_0} \tag{15}$$

And Eq. (13) can be rewritten as:

$$\varepsilon_0 = \theta_1 e^{A\varepsilon_0}\left(1-e^{-\theta_2 e^{(B\varepsilon_0)}t}\right) + \theta_3 e^{C\varepsilon_0}\left(e^{\theta_4 e^{(D\varepsilon_0)}t}-1\right), \tag{16}$$

where A, B, C, and D are parameters that are newly proposed in this study. This paper will refer to the new model as the eight-parameter model, while the model without parameters A and C will be referred to as the six-parameter model, which is the same as the model proposed by Fu et al. [6].

The eight-parameter model can be applied to describe the creep curve obtained under constant load before the point of necking. The model expressed as Eq. (16) includes the creep engineering strain. That means it is impossible to fit the eight parameters as well as to reconstruct the creep curve with only fitted eight parameters without the creep curve obtained from a constant-load creep test. Therefore, the eight-parameter model cannot be used to construct a creep-strain model, but it can be applied to create the constant-stress creep curve from the constant-load creep curve. Compared to the original θ projection method, Eq. (1), the modified method, Eq. (16), uses four added parameters, $A\varepsilon_0$, $B\varepsilon_0$, $C\varepsilon_0$, and $D\varepsilon_0$, to account for the increase of the true stress during the creep process. By removing these parameters, the eight-parameter model can predict the creep curve obtained under constant-stress conditions.

4. Constant-stress creep curves for SG tube material

The previous section introduced a new methodology to obtain the creep curve under constant stress and considering the increase in true stress with creep deformation during the constant-load creep test. The creep curve obtained under constant-stress conditions is necessary to simulate structural behavior for FEA or analytical analysis. In this section, the new methodology is used to generate a constant-stress creep curve from a constant-load creep curve for an SG tube material, alloy 690.

All of the parameters of the eight-parameter model are obtained from the experimental creep curves obtained at a constant temperature and constant load. Suitable parameter values are optimized by minimizing the error between the experimental creep curves and predicted curves calculated using Eq. (16) [24]. Fig. 5 shows a creep curve and creep-strain rate curve at 700 °C and 120 MPa of engineering stress. As shown in Fig. 5(a) and (b), the eight-parameter model suitably fit the creep curve for all stages of the creep process. The six-parameter model also predicted the overall creep well, but these results are not included in Fig. 5(a). As mentioned in the previous section, despite the excellent fit, the creep-strain model cannot be created with this model because the creep curve cannot be reconstructed with only fitting parameters, without the creep test data. However, by removing the four parameters, $A\varepsilon_0$, $B\varepsilon_0$, $C\varepsilon_0$, and $D\varepsilon_0$, the eight-parameter model can predict the constant-stress creep curves. The constant-stress creep curves were presented with six- and eight-parameter models in Fig. 5(a). Also, the eight-parameter model was used to evaluate the effect of the use of a part of creep data on the curve fitting result. The fitting range was defined on time axis, and the meaning was represented in Fig. 5(a). The curve fitting was conducted using 35% of creep curve in the time ranges and 40% of creep curve. In curve fitting using an eight-parameter model, the creep strain was lower than using a six-parameter model. In addition, when a part of creep data below about 40% creep data resulted in a lower constant-stress creep curve than using 100% creep data, the creep strain also decreased as the amount of data used in curve fitting decreased.

FEA was conducted to verify the eight-parameter model. Fig. 6 shows a finite element mesh for the creep specimen. The gauge section was modeled only for the FEA because deformation of the specimen occurred in this particular section during the creep test.

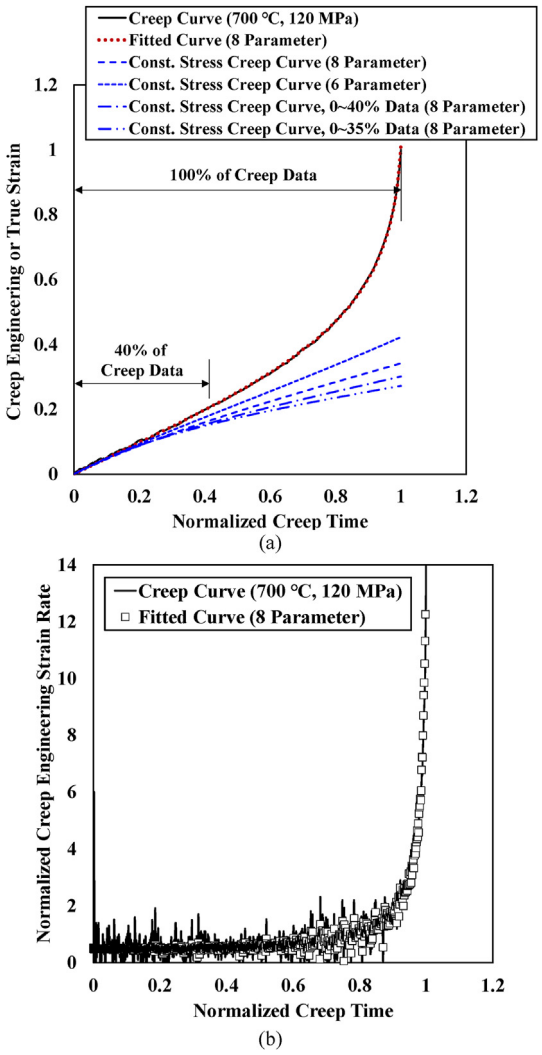

Fig. 5. Curve fitting results for alloy 690 SG tube material obtained based on 8- and 6-parameter models: (a) Normalized creep-strain curve (b) Normalized creep-strain rate curve.

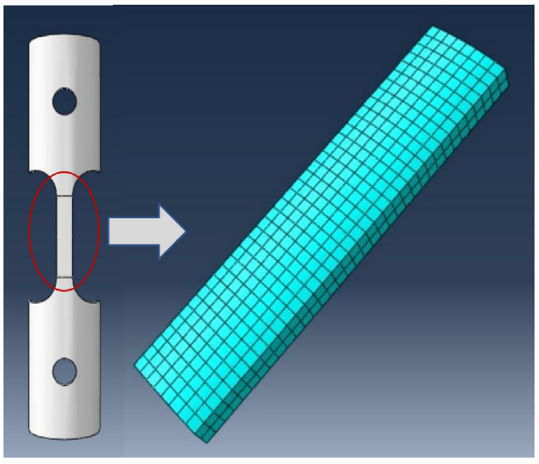

Fig. 6. Schematic diagram and FE mesh for creep test specimen.

The reduced integration eight-node brick element (C3D8R in the ABAQUS element library [25]) was used. The FEA of the creep test was conducted using ABAQUS (version 2018), and the user creep

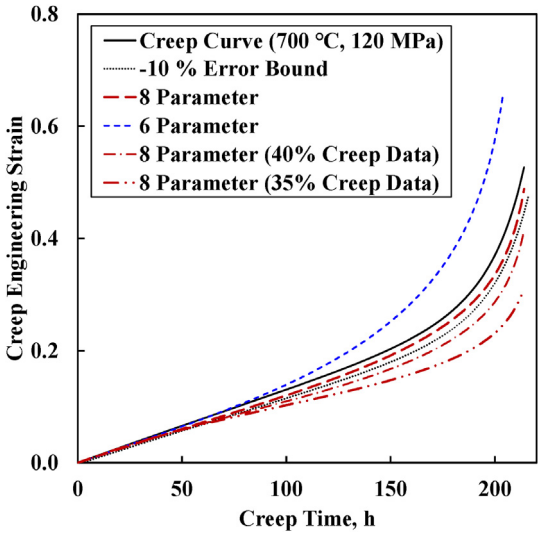

Fig. 7. Simulated constant-load creep curve using constant-stress creep curve.

subroutine was used to apply the newly proposed creep-strain model based on the eight-parameter model. The constant-stress creep curves represented in Fig. 5(a) were used as the input material properties. To simulate constant-load creep experimental conditions, the stress change with increasing creep strain under constant load was calculated using Eq. (9) and used as the input load for FEA.

FEA results for the test conditions of 120 MPa engineering stress at 700 °C were presented in Fig. 7. When using the constant-stress creep curve obtained by the eight-parameter model as an input for the FEA, the constant-load creep test results were predicted within 10%. The difference is that the FEA model does not include a constitutive equation to model damage growth and accumulation in the material. Therefore, we believe that the behavior of the constant-load creep curve simulated using the constant-stress creep curve obtained by the eight-parameter model proposed in this study is reasonable and can be used to evaluate creep behavior without considering the accumulation of the damage in practice. When simulated using a constant-stress creep curve obtained by a six-parameter model, the constant-load creep curve was found to overestimate the creep strain. It is not appropriate for the simulated creep strain to exceed the creep strain of raw data because damage accumulation was not considered during the FEA. Therefore, it is believed that the constant-stress creep curve derived using a six-parameter model is relatively incorrect. Furthermore, when using the eight-parameter model, we confirm that a part of creep data for curve fitting could predict creep strain smaller than that produced from an entire creep curve.

In this paper, the creep-strain model for the constant-stress creep curve of alloy 690 was newly proposed using the eight-parameter model with the same approach as presented in section 2, and the θ parameters are presented in Table 3. Fig. 8 shows the constant-load creep-strain curves from Eq. (3) and the constant-stress creep-strain curves from the eight-parameter model expressed by Eq. (16). The constant-stress creep curves can be applied to evaluate the creep rupture behavior of SG tubes in conjunction with time hardening, strain hardening, and damage-fraction hardening rules. Furthermore, it is believed that more accurate creep behavior of structures can be evaluated by applying the creep-strain model for constant-stress creep in conjunction with the damage accumulation model together in the future.

Table 3
Optimized θ coefficients for the master curve of constant-stress creep curves for alloy 690 SG material.

θ_1	θ_2	θ_3	θ_4	θ_5
0.12	2.40	0.96	0.22	1.0

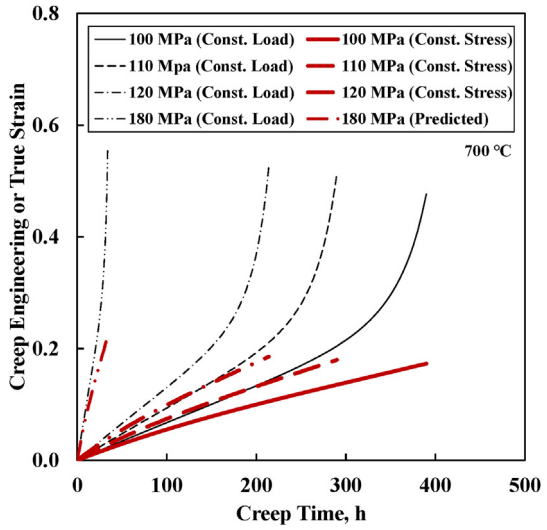

(a)

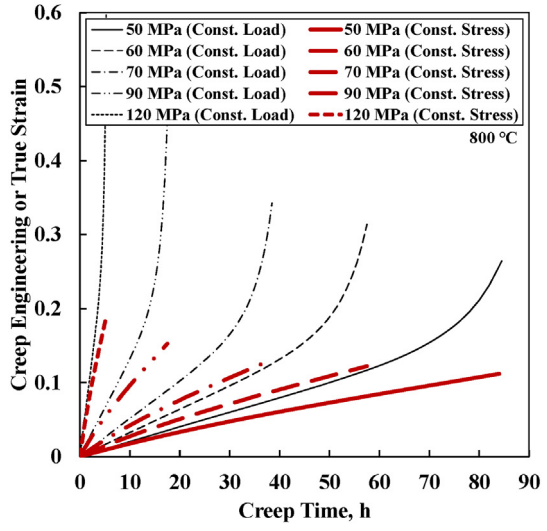

(b)

Fig. 8. Constant-load and -stress creep curves using the creep-strain model for alloy 690 SG tube material.

5. Creep rupture behavior of SG tubes

During a hypothetical accident, SG tubes undergo dynamic changes in pressure and temperature, and the creep damage accumulates within only several hours or, at most, days [15,16]. The creep-strain model presented in the previous section for alloy 690 under constant stress can be applied to predict the creep behavior during an accident. In general, a creep-strain model defined as a function of stress, temperature, and time is insufficient for predicting creep rupture in structures. An assumption must be made as to how the creep behavior is affected by the previous load history. Two rules are often used: time hardening and strain hardening [6–8,26]. A third methodology, named damage-fraction hardening, was proposed in this paper.

Time hardening assumes that creep-strain rate depends only on the time from the beginning of the creep process and ignores the quantity of creep strain experienced in the previous history. In contrast, strain hardening assumes that the creep-strain rate depends only on the current creep strain. These methods were graphically illustrated in Fig. 9 for the stress history shown in Fig. 9(a). Estimated strains are shown in Fig. 9(b) and (c) for the two rules. For time hardening and strain hardening, whenever the stress changes, the deformation is assumed to proceed according to the curve for the new stress, starting at the point on this curve corresponding to the actual values of time and strain, respectively.

In this study, a damage-fraction hardening rule was proposed, and Fig. 9(d) shows the concept of the damage-fraction hardening rule. As described in Section 2, all the creep curves for alloy 690 SG tube material can be converged on a single curve by being normalized with the reference creep rupture time and strain, expressed by Eqs. (5) and (6), respectively, and then a master curve can be determined. It can be assumed the creep failure occurs at the normalized creep strain in the master curve reaches at 1.0, and the normalized strain is defined as the damage. From the master curve the equivalent damage can be determined for all specific creep curves. The damage contour lines in Fig. 9(d) can be determined from the creep-strain master curve so that when the stress changes, it is possible to proceed from the prior creep curve to current creep curve along the equivalent damage path as shown Fig. 9(d). Therefore, in the damage-fraction hardening, the creep-strain rate depends only on the current total creep damage-fraction. From Fig. 9, it can be found that the predicted creep rupture pressure with the strain hardening rule will accumulate the most damage, and the one with the time hardening rule will have the smallest accumulation of damage. Thus, it can be inferred that the creep hardening rules predict the creep rupture pressure is high for the strain hardening rule, damage-fraction hardening rule, and strain hardening rule.

The three hardening models were applied to predict the creep rupture of an SG tube. Next, the prediction results were compared with the creep rupture test results. The rupture tests were conducted at 700 and 800 °C with a pressure ramp rate of 23 psi/min. The tube specimen is 540 mm long, 19.05 mm outside diameter, and 1.07 mm thick, and was designed to have an axial part through-wall defect of which depth is 60 or 80% of the wall thickness. The creep rupture test results are tabulated in Table 4.

The creep rupture of the tube can be predicted using the applied stress in crack ligament and creep hardening rules. The stress of the axial part-through-wall crack ligament can be calculated using the following equation [2,27], which is based on the flow stress model.

$$\sigma = \frac{m_p R_m P}{h}, \tag{17}$$

where P is applied internal pressure, R_m is mean tube radius, h is tube wall thickness, and m_p is defined as follows:

$$m_p = \frac{1 - \alpha \frac{a}{mh}}{1 - \frac{a}{h}}, \tag{18}$$

where a is crack depth and, α is defined as follows:

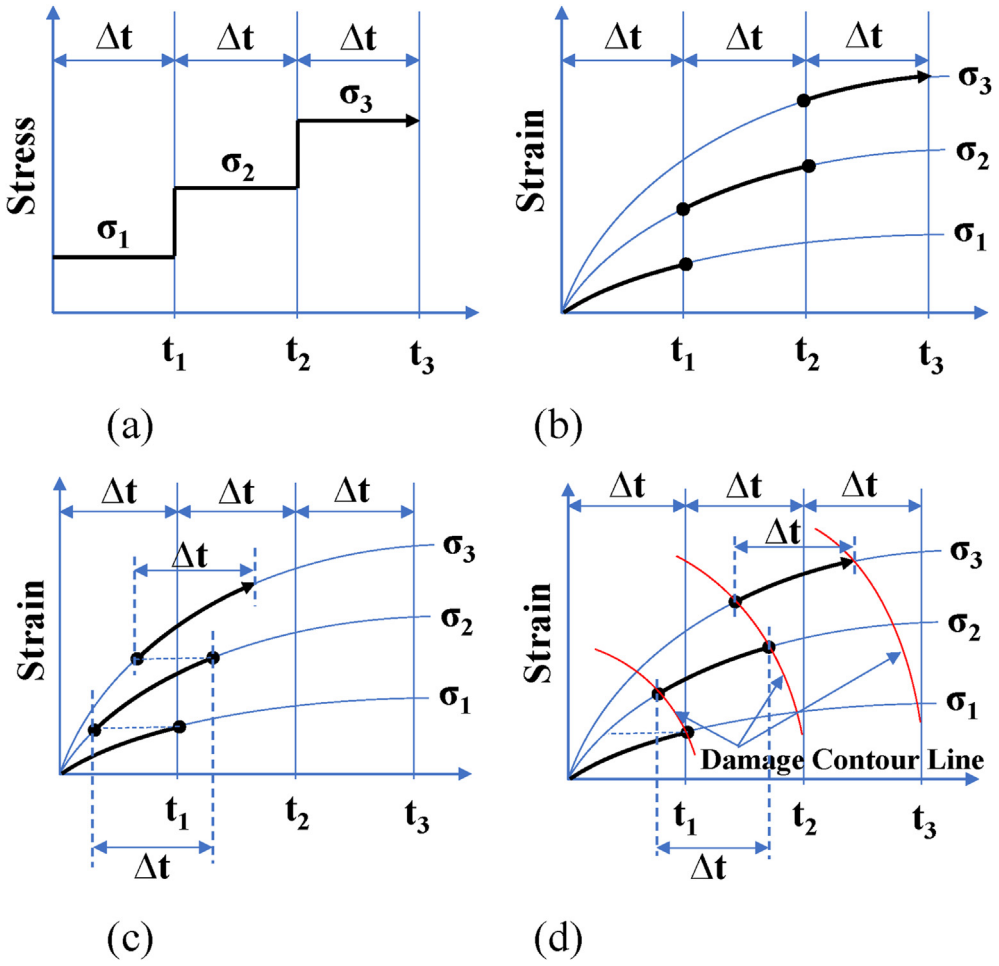

Fig. 9. Schematics showing creep hardening rules: (a) load history, (b) time hardening rule, (c) strain hardening rule, and (d) damage-fraction hardening rule.

Table 4
Results of alloy 690 tube rupture test and prediction.

Test ID	Temperature (°C)	Flaw Depth (%)	Rupture Pressure (MPa)	Predicted Rupture Pressure by Time Hardening (MPa)	Predicted Rupture Pressure by Strain Hardening (MPa)	Predicted Rupture Pressure by Damage-fraction Hardening (MPa)
1	700	60	19.2	16.2	22.3	20.2
2	800	60	10.8	9.3	13.6	12.0
3	700	80	12.9	9.7	13.2	12.1
4	800	80	6.5	5.7	8.1	7.3

$$\alpha = 1 + 0.9\left(\frac{a}{h}\right)^2\left(1 - \frac{1}{m}\right), \tag{19}$$

$$m = 0.614 + 0.481\lambda + 0.386e^{(-1.25\lambda)}, \tag{20}$$

$$\lambda = \left[12\left(1-\nu^2\right)\right]^{1/4}\frac{c}{\sqrt{R_m h}} = \frac{1.82c}{\sqrt{R_m h}}, \tag{21}$$

where c is crack half-length.

The creep behaviors of the SG tube evaluated using time hardening, strain hardening, and damage-fraction hardening rules are presented in Fig. 10. It was assumed that the creep rupture of the tube occurs when the creep strain in crack ligament reaches the creep rupture strain, expressed by Eq. (6). As expected, the predicted creep rupture pressure of an SG tube with an axial part-through-wall defect was the lowest using the time hardening rule and the highest using the strain hardening rule. As shown in Fig. 10, the predicted creep behavior using the strain hardening rule is more similar to that using the damage-fraction hardening rule than that using the time hardening rule. However, it shows a significantly higher creep strain near the point of rupture. Also, the creep strain was very low under low applied pressure in all cases. For example, when the damage-fraction rule was applied, even when the pressure reached 15.7 MPa, it was just 10% of the creep strain at the time of rupture (20.2 MPa). Because of this, the accumulated amount of creep damage under relatively lower pressure conditions was considered insignificant.

Fig. 11 and Table 4 show the comparison of experimental and predicted results. Overall, the results predicted using the time hardening rule were conservative, but the results predicted using the strain hardening rule were nonconservative. The results using the damage-fraction hardening rule were consistent with the

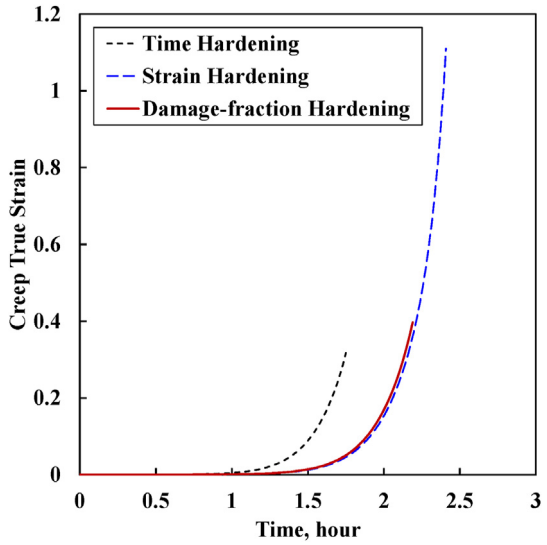

Fig. 10. Comparison of predicted creep rupture behaviors using creep hardening rules.

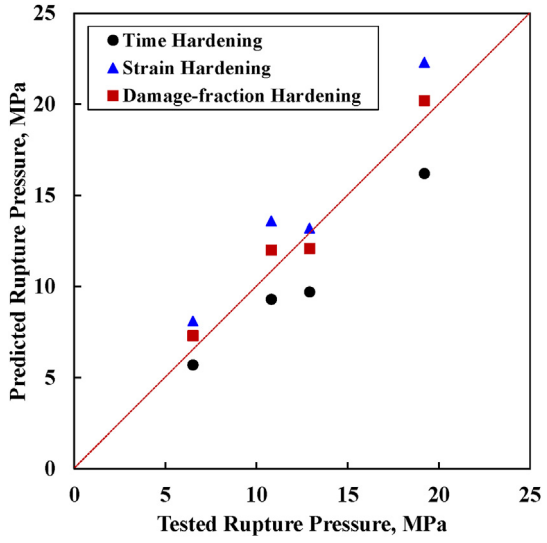

Fig. 11. Comparison of tested rupture pressure and predicted rupture pressure using strain hardening rules.

experimental results. Therefore, it is confirmed that the creep-strain model for alloy 690 and the damage-fraction hardening rule proposed can be used to predict the creep rupture of an SG tube in a hypothetical nuclear power plant.

6. Conclusion

A novel methodology was proposed to obtain the constant-stress creep curve from the constant-load creep curve. The methodology, named the eight-parameter model, is based on a modified θ projection method and considers the increase in true stress with creep deformation during a constant-load creep test. The eight-parameter model was validated using finite element analysis (FEA) by simulating the constant-load creep test process. The creep-strain model for the constant-stress creep curve of alloy 690 was proposed using the eight-parameter model. Moreover, the novel damage-fraction hardening rule was proposed. The utility of the damage-fraction model was validated by applying the damage-fraction hardening rule to evaluate the creep rupture behavior of SG tubes with an axial part-through-wall defect. The results of this study show great potential to evaluate SG tube creep rupture behavior in a severe accident governed by creep deformation. It is believed that a more accurate creep behavior of SG tubes will be possible by applying the damage accumulation model with FEA and the constant-stress creep curve in the future.

Declaration of competing interest

The authors declare that they have no known competing financial interests or personal relationships that could have appeared to influence the work reported in this paper.

Acknowledgments

This work was supported by a National Research Foundation of Korea (NRF) grant funded by the Korean government (MIST) (2017M2A84015156).

References

[1] S. Sancaktar, M. Salay, R. Lyengar, A. Azarm, S. Majumdar, Consequential SGTR analysis for westinghouse and combustion engineering plants with thermally treated alloy, Steam Generator Tubes 600 (2016), 690, NUREG-2195.
[2] Idaho National Engineering Laboratory, Risk assessment of severe accident-induced steam generator tube rupture, NUREG 1570 (1998).
[3] S. Majumdar, W.J. Shack, D.R. Diercks, K. Mruk, J. Franklin, L. Knoblich, Failure behavior of internally pressurized flawed and unflawed steam generator tubing at high temperatures—experiments and comparison with model predictions, NUREG/CR 6575 (1998).
[4] S. Majumdar, Prediction of structural integrity of steam generator tubes under severe accident conditions, Nucl. Eng. Des. 194 (1999) 31–55.
[5] J. Kim, W. Kim, C. Kim, Evaluation of Creep Properties of Alloy 690 Steam Generator Tubes at High Temperature Using Tube Specimen, ASME 2019 Pressure Vessels and Piping Conference, 2019. PVP2019-93498.
[6] A.S. Krausz, K. Krausz, Unified Constitutive Laws of Plastic Deformation, Academic Press, 1996, pp. 107–152.
[7] N.E. Dowling, Mechanical Behavior of Materials, Prentice Hall, 1999.
[8] P. Yu, W. Ma, A modified theta projection model for creep behavior of RPV steel 16MND5, J. Mater. Sci. Technol. 47 (2020) 231–242.
[9] R. Pohja, S. Holmström, H.Y. Lee, Strain and Damage-Based Analytical Methods to Determine the Kachanov-Rabotnov Tertiary Creep-Damage Constants, Brown University, 2012.
[10] M.S. Haque, C.M. Stewart, Comparative analysis of the sin-hyperbolic and Kachanov-Rabotnov creep-damage models, Int. J. Pres. Ves. Pip. 171 (2019) 1–9.
[11] V.S. Srinivasan, B.K. Choudhary, M.D. Mathew, T. Jayakumar, Creep behaviour of 9Cr-1Mo ferritic steel using theta-projection approach and evolution of a damage criterion, Trans. SMiRT 21 (Div–I) (2011). Paper, ID# 779.
[12] C. Fu, Y. Chen, X. Yuan, S. Tin, S. Antonov, K. Yagi, Q. Feng, A modified θ projection model for constant load creep curves-I. Introduction of the model, J. Mater. Sci. Technol. 35 (2019) 223–230.
[13] D.L. May, A.P. Gordon, The application of the Norton-bailey law for creep prediction through power law regression, Proc. ASME Turbo Expo (2013). GT2013-96008.
[14] J.M. Montes, F.G. Cuevas, J. Cintas, New creep law, Mater. Sci. Technol. 28 (2012) 377–379.
[15] B. Derby, M.F. Ashby, Power-laws and A-n correlation in creep, Scripta Metall. 18 (1984) 1079–1084.
[16] B.S. Lee, J.M. Kim, J.Y. Kwon, K.J. Choi, M.C. Kim, A practical power law creep modeling of alloy 690 SG tube materials, Nucl. Eng. Technol. (2021). Available Online.
[17] P.E. MacDonald, V.N. Shah, L.W. Ward, P.G. Elliso, Steam Generator Tube Failures, U.S. NRC, 1996. NUREG/CR-6365.
[18] K.J. Karwoski, G.L. Maker, M.G. Yoder, U.S. Operating Experience with Thermally Treated Alloy 690 Steam Generator Tubes, U.S., NRC, 2007. NUREG-1841.
[19] R.W. Evans, L. Beden, B. Wilshire, On Creep and Fracture of Engineering Materials and Structures, Pineridge Press, Swansea, 1984, p. 1277.
[20] ECCC, Recommendations and guidance for the assessment of creep strain and creep strength data, ECCC Recommend. 5 (2003) 38.
[21] W. Harrison, Z. Abdallah, M. Whittaker, A model for creep and creep damage in the γ-titanium aluminide Ti-45Al-2Mn-2Nb, Materials 7 (2014) 2194–2209.
[22] C. Fu, Y. Chen, X. Yuan, S. Tin, S. Antonov, K. Yagi, Q. Feng, A modified θ projection model for constant load creep curves-II. Application of creep life prediction, J. Mater. Sci. Technol. 35 (2019) 687–694.

[23] S. Moon, J.M. Kim, J.Y. Kwon, B.S. Lee, K.J. Choi, M.C. Kim, Creep strain modeling for alloy 690 SG tube material based on modified theta projection method, Nucl. Eng. Technol., In Review..
[24] R.W. Evans, Statistical scatter and variability of creep property estimates in θ projection method, Mater. Sci. Technol. 5 (1989) 699–707.
[25] Dassault, ABAQUS version 6.14. User's Manual, Dassault Systems Simulia, 2018.
[26] W.D. Day, A.P. Gordon, Life fraction hardening applied to a modified theta projection creep model for a Nickel-based super-alloy, Proc. ASME Turbo Expo (2014). GT2014-25881, 2014.
[27] S. Moon, Y.S. Chang, Y.J. Kim, J.H. Lee, M.H. Song, Y.H. Choi, S.S. Hwang, Assessment of plastic collapse behavior for tubes with collinear cracks, Eng. Fract. Mech. 73 (2006) 296–308.